Human Molecular Genetics, 2014, Vol. 23, No. 10 **2769–2779**
doi:10.1093/hmg/ddt672
Advance Access published on January 2, 2014

Polycystin-1 regulates actin cytoskeleton organization and directional cell migration through a novel PC1-Pacsin 2-N-Wasp complex

Gang Yao[1], Xuefeng Su[1], Vy Nguyen[1], Kristina Roberts[1], Xiaogang Li[1], Ayumi Takakura[1], Markus Plomann[2] and Jing Zhou[1,*]

[1]Center for Polycystic Kidney Disease Research and Renal Division, Department of Medicine, Brigham and Women's Hospital, Harvard Medical School, Boston, MA 02115, USA [2]Center for Biochemistry, University of Cologne, Joseph-Stelzmann-Str. 52, Cologne 50931, Germany

Received November 21, 2013; Revised and Accepted December 30, 2013

How epithelial cells form a tubule with defined length and lumen diameter remains a fundamental question in cell and developmental biology. Loss of control of tubule lumen size in multiple organs including the kidney, liver and pancreas features polycystic kidney disease (PKD). To gain insights into autosomal dominant polycystic kidney disease, we performed yeast two-hybrid screens using the C-terminus of polycystin-1 (PC1) as bait. Here, we report that PC1 interacts with Pacsin 2, a cytoplasmic phosphoprotein that has been implicated in cytoskeletal organization, vesicle trafficking and more recently in cell intercalation during gastrulation. PC1 binds to a 107-residue fragment containing the α3 helix of the F-BAR domain of Pacsin 2 via a coiled-coil domain in its C-tail. PC1 and Pacsin 2 co-localize on the lamellipodia of migrating kidney epithelial cells. PC1 and Pacsin 2-deficient kidney epithelial cells migrate at a slower speed with reduced directional persistency. We further demonstrate that PC1, Pacsin 2 and N-Wasp are in the same protein complex, and both PC1 and Pacsin 2 are required for N-Wasp/Arp2/3-dependent actin remodeling. We propose that PC1 modulates actin cytoskeleton rearrangements and directional cell migration through the Pacsin 2/N-Wasp/Arp2/3 complex, which consequently contributes to the establishment and maintenance of the sophisticated tubular architecture. Disruption of this complex contributes to cyst formation in PKD.

INTRODUCTION

Most major organs in a human body, including the lung, kidney, liver and mammary glands and vasculature, are composed primarily, sometimes exclusively, of tubules. A tubule formed by epithelia or endothelia has strictly controlled length and diameter, which are essential for its specified function. Polycystic kidney disease (PKD) is a pathological condition in which such control is lost in the kidney, liver and pancreas, leading to cyst formation. The autosomal dominant form of PKD (ADPKD) is the most common life-threatening genetic disease in humans, affecting 1 in 500–1000 live births. Kidney dialysis and organ replacement are the only current therapies for patients with renal failure (1,2).

Polycystin-1 (PC1) and polycystin-2 (PC2) are proteins, respectively, encoded by *PKD1* and *PKD2* (2,3). Mutations in *PKD1* cause ∼85% of ADPKD cases (4). PC1 is a large (∼4302 residues) integral membrane protein with 11 transmembrane domains. The extracellular part of PC1 contains multiple domains that may serve for ligand binding, cell–cell or cell–matrix interactions (5–8). The cytoplasmic tail of PC1 mediates intracellular signal transduction probably through binding to PC2 ion channel and heterotrimeric G proteins (3,9–13). The expression of *Pkd1* is higher in both mRNA and protein levels in embryonic kidneys when there is active cell migration, than in fully developed adult kidneys (14,15). PC1 overexpression has been reported to regulate cell migration through PI3 kinase-dependent cytoskeletal rearrangement and GSK3-dependent cell–cell adhesion in MDCK cells (16).

Pacsin 2 is a member of the Pacsin (protein kinase C and casein kinase 2 substrate in neurons) protein family that contains a highly conserved Src-homology 3 (SH3) domain. To date,

*To whom correspondence should be addressed at: Harvard Institutes of Medicine, Room 522, 4 Blackfan Circle, Boston, MA 02115, USA. Tel: +1 6175255860; Fax: +1 6175255830; Email: jzhou@partners.org; zhou@rics.bwh.harvard.edu

there are three known members in the Pacsin protein family. Pacsin 1 localizes specifically to neurons, Pacsin 3 is mainly detected in lung and muscle, whereas Pacsin 2 has a ubiquitous distribution (17–19). Pacsins localize to sites of high actin turnover, such as filopodia tips and lamellipodia (20), and directly interact via their SH3 domains with the neural Wiskott–Aldrich syndrome protein (N-Wasp) (18), a potent activator of the Arp2/3 complex which functions in cell migration and in actin filament nucleation (20–22). The latter function is the rate limiting step for actin filament polymerization (23). Pacsins were reported to be required for convergent extension movements during gastrulation in frogs and zebrafish (24,25). Most recently, we showed that Pacsin 2 expression is nephron segment specific and is regulated during kidney development, and injury and repair. Pacsin 2 knockdown mouse inner medullary collecting duct (mIMCD3) cells exhibit remarkable tubulogenic defects in 3D culture (26), which suggests that Pacsin 2 may contribute to the formation and maintenance of normal kidney tubular structures.

In this study, we show that PC1 interacts with Pacsin 2. Loss of PC1 leads to disorganized actin cell cytoskeleton and alters the localization of Pacsin 2 in kidney epithelial cells. Wound-healing analysis and live cell imaging of random cell migration revealed that both *Pkd1*-deficient and *Pacsin 2*-depleted kidney epithelial cells migrated at a slower speed with a reduced directional persistency. We further demonstrate that PC1, Pacsin 2 and N-Wasp are in the same protein complex and that PC1 and Pacsin 2 are essential for the proper binding ability of N-Wasp to Arp3. This binding is necessary for the activity of the Arp2/3 complex in actin filament nucleation. Consistently, *Pkd1*-deficient cells display reduced abundance of Pacsin 2 and Arp3 in lamellipodia during migration. Because directional cell migration is required for tubulogenesis both *in vitro* and *in vivo*, we propose that the PC1-Pacsin 2-N-Wasp protein complex identified in this study is necessary in the establishment and maintenance of actin cytoskeleton organization in tubular epithelial cells.

RESULTS

Identification of Pacsin 2 as a novel PC1-interacting protein

To understand proximal molecular events mediated by PC1, we performed yeast two-hybrid screens with the human PC1 C-terminal intracellular domain (ICD) (residues 4079–4302) as bait and isolated Pacsin 2 as a candidate from a human fetal kidney library. Yeast co-transformation of PC1-ICD with three Pacsin 2 truncation mutants (Pacsin 2^{1-170}, Pacsin $2^{171-278}$ and Pacsin $2^{279-486}$) that express the N-terminal, middle and C-terminal region of Pacsin 2, respectively, showed that only the Pacsin $2^{171-278}$ fragment is able to bind the PC1-ICD (Fig. 1A). This fragment contains the α3 helix of the Fer-CIP4 homology-Bin-Amphiphysin-Rvs (F-BAR) domain (184–239 amino acids), which is conserved within the Pacsin protein family (27).

To confirm the interaction in mammalian cells, we determined the expression of Pacsin 2 in kidney epithelial cells. Pacsin 2 antibodies coimmunoprecipitated endogenous Pacsin 2 and PC1 in collecting duct originated (purified with dolichos biflorus agglutinin, DBA) mouse embryonic kidney (MEK) epithelial cells, confirming that PC1 and Pacsin 2 are present in the same protein complex (Fig. 1B).

To further verify whether Pacsin 2 interacts with PC1, either GST-human PC1 C-tail (residues 4105–4302) fusion peptides (GST-hPC1-ICD) (28) or control GST peptide alone were immobilized on glutathione sepharose beads and incubated with MEK DBA^+ cell lysates. The GST-PC1 fusion peptides, but not GST alone, were able to pull-down endogenous Pacsin 2 in the MEK DBA^+ cell lysates (Fig. 1C). The interaction was also confirmed in the opposite direction. GST-full-length Pacsin 2 fusion peptides (GST-Pacsin 2) but not GST alone were able to pull-down PC1 (Fig. 1D) from a tetracycline-inducible PC1 stable cell line (293T-PC1S) described previously (29,30).

To determine the Pacsin 2-binding domain in PC1 C-tail, we performed a GST pull-down assay using GST-Pacsin 2 and various CD16.7 tagged C-terminal cytoplasmic tail of PC1 proteins that were transiently expressed in 293 cells (Supplementary Material, Fig. S1B). While the full-length C-terminal tail of PC1 (CD16.7-ICD) and the N-terminal truncation mutant PC1 C-tail (CD16.7-112) that contain the G-protein activation domain interacted well with GST-Pacsin 2, the coiled-coil deletion mutant (CD16.7-112ΔCC) completely lost its ability to bind to GST-Pacsin 2, suggestive of a critical role of PC1 coiled-coil domain in recognizing Pacsin 2. In addition, the C-terminal truncation mutant CD16.7-112Δ54 that does not have the last 54 amino acids of the PC1-C-tail also manifested a remarkable reduced binding capacity to GST-Pacsin 2. To further confirm that Pacsin 2 interacts with full-length PC1 through binding to the coiled-coil domain in PC1-C-tail, we engineered a pathogenic mutation (Q4215P that interrupts the coiled-coil domain (31)) found in human ADPKD patients into full-length PC1 and used GST-Pacsin 2 to pull down either wild-type YFP-tagged full-length PC1 or this mutant PC1 transiently expressed in 293 cells. As expected, the GST-Pacsin 2 efficiently pulled down wild-type full-length PC1, but not the coiled-coil domain mutant PC1 (YFP-PC1-Q4215P) (efficiency reduced by ∼10-fold). Interestingly, the YFP-PC1-R3269C, another pathogenic, hypomorphic mutation we engineered in the first intracellular loop of PC1 (32,33) also showed a remarkably reduced interaction with GST-Pacsin 2 (Fig. 1E; see Supplementary Material, Fig. S1A for a longer exposure image).

These results indicate that the coiled-coil domain in the C-terminal intracellular tail of PC1 is necessary for PC1 to interact with Pacsin 2. In addition, PC1 mutations that are outside of the coiled-coil domain, such as the one in the first intracellular loop (R3269C) or those in the last 54 amino acids (immediate C-terminal to the coiled-coil domain) may also affect the interaction between the PC1-ICD and the α3 helix of the F-BAR domain in Pacsin 2.

Pacsin 2 co-localizes with PC1 in lamellipodia

We next investigated whether PC1 and Pacsin 2 are co-localized. Because of the lack of PC1-specific antibody for immunostaining, we stained YFP-PC1 and endogenous Pacsin 2 in an mIMCD3 cell line stably expressing YFP-PC1. As seen in Figure 1F, YFP-PC1 co-localizes with Pacsin 2 in the cell body, lamellipodium and especially at the leading edge. The co-localization of YFP-PC1 with Pacsin 2 is significantly enhanced in the presence of PC2-HA,

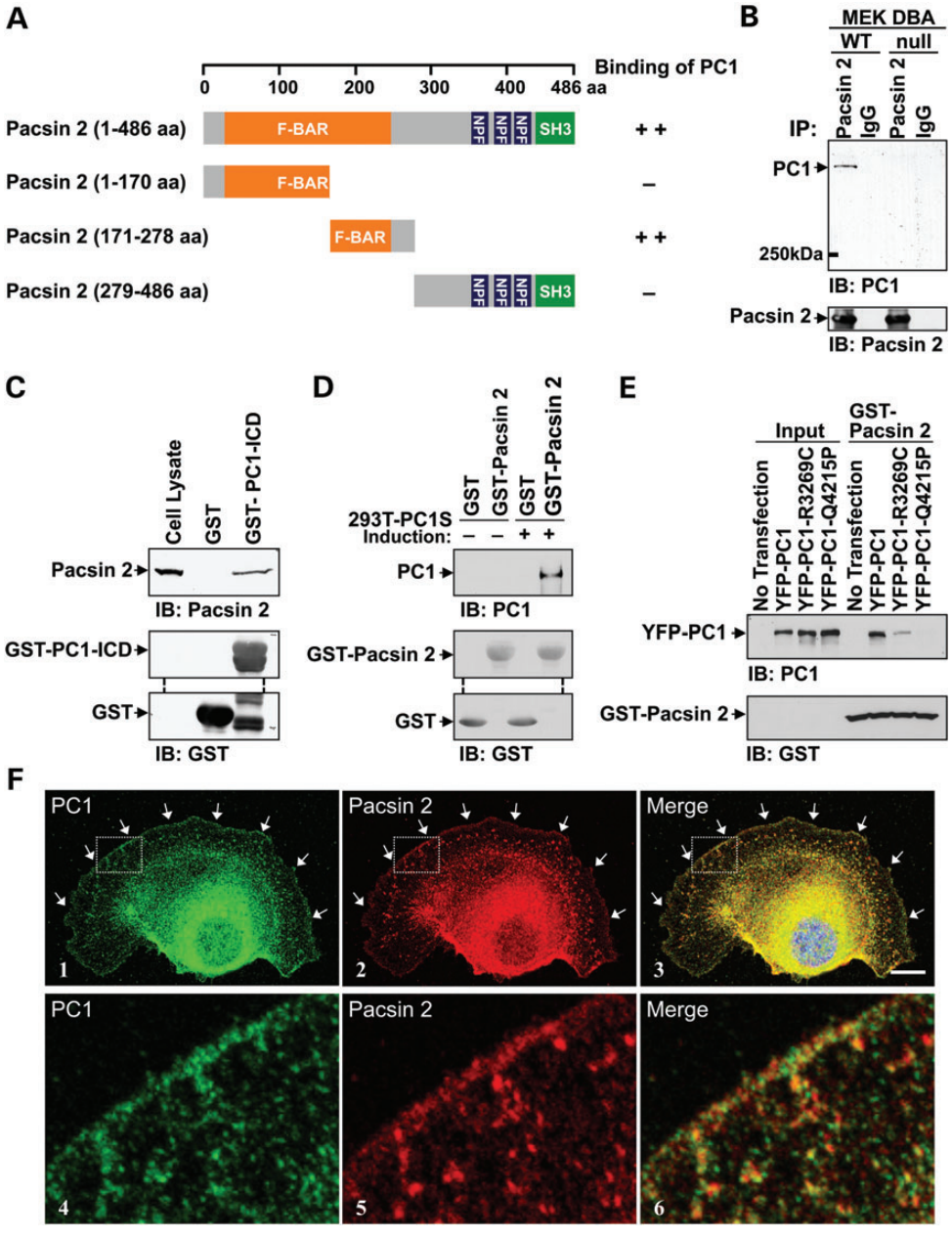

Figure 1 Pacsin 2 interacts with PC1 in yeast and renal epithelial cells. (**A**) A scheme showing the interaction between Pacsin 2 and the PC1 C-terminal in yeast. F-BAR stands for the Fer-CIP4 homology-Bin-Amphiphysin-Rvs domain. NPF stands for the asparagine-proline-phenylalanine motif. SH3 stands for the SH3 domain. (**B**) Endogenous Pacsin 2 and PC1 co-immunoprecipitate (IP) in MEK DBA^{+} *Pkd1*$^{+/+}$ (WT) but not in *Pkd1*$^{null/null}$ (null) cells. (**C**) GST-PC1-ICD pulls down endogenous Pacsin 2 from the MEK DBA^{+} *Pkd1*$^{+/+}$ cell lysates. (**D**) GST-Pacsin 2 pulls down exogenous PC1 from the tetracycline-induced 293T-PC1S cell lysates. (**E**) Interaction of GST-Pacsin 2 with mutant full-length PC1-Q4215P or R3269C is greatly reduced, when compared with wild-type PC1. Input is 1/10 of cell lysates used for pull-down experiments. (**F**) Confocal image showing that YFP-PC1 and endogenous Pacsin 2 co-localize on lamellipodia of mIMCD3 cells stably expressing YFP-PC1. Panels 4–6 are enlarged images of the inserts of boxed areas 1–3, respectively. Arrows point to the lamellipodium. Scale bar stands for 10 μm.

which increases the plasma membrane expression of PC1 (34) (result not shown).

PC1, Pacsin 2 and N-Wasp are in the same protein complex

Pacsin 2 directly interacts with N-Wasp and functions in the Arp2/3-dependent actin nucleation (18). Because deficiency in PC1, Pacsin 2 or N-Wasp causes defects in tubulogenesis in kidney epithelial cells in 3D cell culture (26,35,36), we hypothesized that Pacsin 2 binds both PC1 and N-Wasp allowing the signals received by PC1 to be transmitted to N-Wasp and to regulate the Arp2/3 complex activity. We tested this hypothesis by immunoprecipitation of N-Wasp in cell lines with either PC1 deficiency or Pacsin 2 depletion. Endogenous PC1 and Pacsin 2 were co-immunoprecipitated with N-Wasp in control mIMCD3 and MEK cells, but not in Pacsin 2

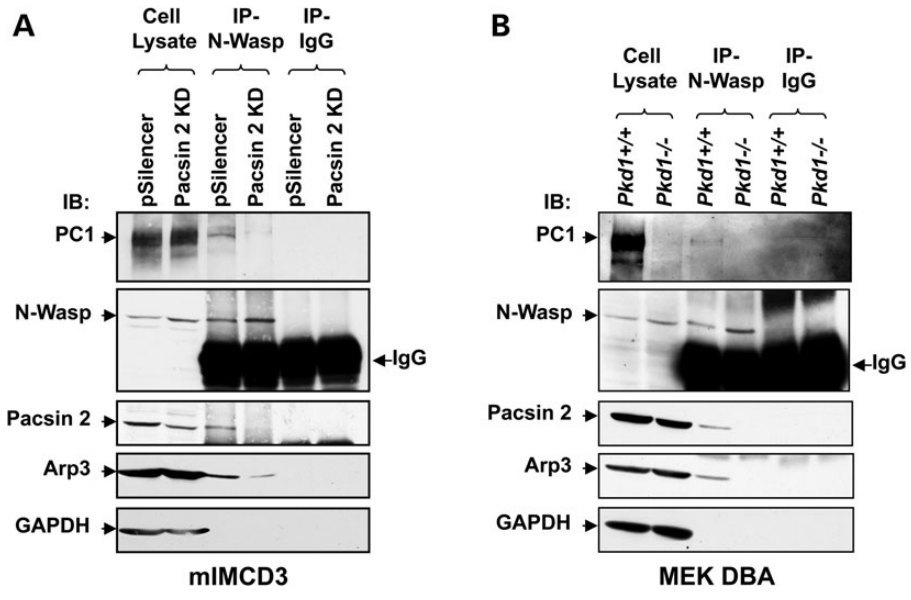

Figure 2 PC1, Pacsin 2 and N-Wasp are found in one protein complex. Endogenous N-Wasp co-immunoprecipitates endogenous Pacsin 2, PC1 and Arp3 in mIMCD3 cells (**A**) and MEK DBA^{+} cells (**B**). This complex is disrupted in Pacsin 2 knockdown or PC1 *Pkd1*$^{null/null}$ MEK cells.

knockdown mIMCD3 cells (Fig. 2A and B). These data suggest that Pacsin 2 is required to keep PC1 and N-Wasp in one complex. In MEK DBA^{+} *Pkd1*$^{null/null}$ cells, N-Wasp could barely co-immunoprecipitate Pacsin 2 when compared with that in control cells (Fig. 2B). N-Wasp also co-immunoprecipitated Arp3 in both control mIMCD3 and MEK cells (Fig. 2A and B). Its binding ability to Arp2/3, however, was decreased in both Pacsin 2 knockdown mIMCD3 cells and MEK DBA^{+} *Pkd1*$^{null/null}$ cells. Thus, in addition to Pacsin 2, PC1 also regulates actin nucleation activity of Arp2/3 complex via N-Wasp.

PC1 is required for proper actin cytoskeleton formation and lamellipodial localization of Pacsin 2 and Arp3

PC1 overexpression leads to cytoskeletal rearrangements and induces cell migration and tubule formation (16,37,38). To assess the effects of PC1 mutation on the actin cytoskeleton *in vivo*, we stained wild-type (*Pkd1*$^{Flox/Flox}$) and *Pkd1*-deficient (Ubc.Cre.*Pkd1*$^{Flox/Flox}$) mouse kidneys with rhodamin-labeled phalloidin. We found strong F-actin signals decorated the apical membrane with some weak signals outline the tubules in wild-type kidneys (Fig. 3A). In striking contrast, the actin cytoskeleton became remarkably reduced and disorganized in littermate *Pkd1*-deficient (Ubc.Cre.*Pkd1*$^{Flox/Flox}$) kidneys. The typical apical and basal F-actin signals seen in wild-type mouse were replaced by irregular and fibrillar-like structures (Fig. 3A), suggesting that defective actin cytoskeleton is a feature of ADPKD.

Consistent with the disorganization of actin cytoskeleton in *Pkd1*-deficient kidneys *in vivo*, PC1 deficiency led to actin cytoskeleton disorganization, as visualized by phalloidin staining in confluent and differentiated MEK DBA^{+} *Pkd1*$^{null/null}$ cells (Supplementary Material, Fig. S2A), in contrast to the typical epithelial cobblestone pattern of MEK wild-type cells in *in vitro* cell cultures. Under undifferentiated conditions, the MEK *Pkd1*$^{null/null}$ cells spread poorly and possess defective lamellipodia. Although these cells seem to have more stress fibers in the cell body, there are fewer actin filaments decorating the lamellipodia (Supplementary Material, Fig. S2B).

Actin filament polymerization is the underlying force for cell migration. We found that, during wound-healing analysis, MEK *Pkd1*$^{null/null}$ cells migrated slower (Fig. 3B, Supplementary Material, Fig. S3) and had smaller and irregular cellular processes at the migration front (Fig. 3C, arrows) instead of lamellipodia in wild-type cells.

By immunostaining sub-confluent wild-type and *Pkd1*-deficient MEK cells, we found that the Pacsin 2 signals are reduced at the leading edge of the lamellipodia in *Pkd1*-deficient cells and became more diffusely localized in the lamellipodia (Supplementary Material, Fig. S2C). This difference became more obvious during a wound-healing analysis when there is more active cell migration (Fig. 3D). Although no obvious changes in N-Wasp were observed, the Arp3 signal was reduced from the leading edge of lamellipodia in MEK *Pkd1*$^{null/null}$ cells when compared with controls (Fig. 3D), further supporting a defect in actin nucleation by the Arp2/3 complex in these cells.

PC1 and N-Wasp in lamellipodial formation in Pacsin 2-depleted cells

Although the knockdown of Pacsin 2 in fibroblasts and cancer cells promotes cell migration (39,40), Pacsin 2 knockdown kidney epithelial cells migrate slower than control cells in a wound-healing assay (Fig. 4A, Supplementary Material, Fig. S4A). During the 6-h observation time, control mIMCD3 cells migrated at a speed of ~38 μm/h, while Pacsin 2 knockdown cells migrated at ~25–29 μm/h ($n = 6$ for each cell line). Five hours after scratching, cells were fixed and the actin cytoskeleton was visualized by rhodamine-phalloidin. Control

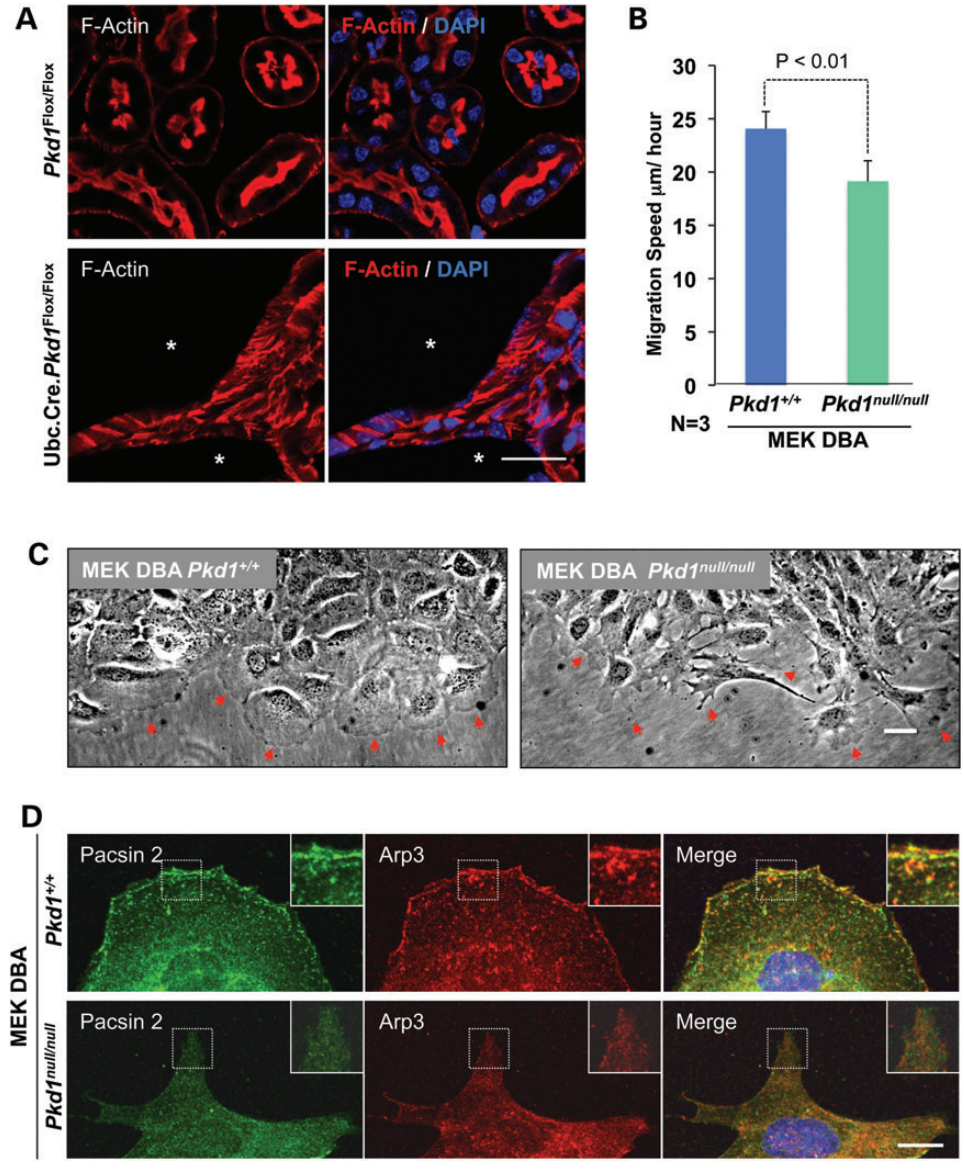

Figure 3 PC1 is required for the integrity of actin cytoskeleton and for cell migration. (**A**) Rhodamine-labeled phalloidin staining shows that strong F-actin signals on the apical and basal membranes in the wild-type (*Pkd1*$^{Flox/Flox}$) mouse kidney tubules. In contrast, the actin cytoskeleton becomes disorganized and apical–basal localization is replaced by stress fibers at the cell–cell junction and within the cell bodies in littermate *Pkd1*-deficient (Ubc.Cre.*Pkd1*$^{Flox/Flox}$) kidney tubules. Asterisk indicates the cysts. Scale bar stands for 50 µm. (**B**) Graphs represent cell migration speed of wild-type and *Pkd1*-deficient MEK cells during the initial 9 h after scratching in three individual wound-healing experiments. (**C**) MEK DBA^{+} *Pkd1*$^{null/null}$ cells form smaller and irregular cellular processes at the migration front. Arrows point to the lamellipodia or irregular cellular processes at migration front. (**D**) Pacsin 2 and Arp3 signals on the lamellipodia, particularly at the leading edge, of *Pkd1* mutant cells are reduced, when compared with control cells in a wound-healing assay. Images were taken 5 h after scratching. Scale bar stands for 10 µm.

cells formed multiple lamellipodia along the wound, which often connected with each other as the filopodia protruded forward. Pacsin 2 knockdown cells, however, formed fewer, often isolated and defective lamellipodia, as well as fewer filopodia (Fig. 4B; Supplementary Material, Fig. S4B), suggesting a defect in the formation of lamellipodia and filopodia in Pacsin 2 knockdown cells.

Although there were no obvious changes in YFP-PC1 and N-Wasp localization in the lamellipodia of Pacsin 2 knockdown cells, the lamellipodial Arp3 signal was reduced in the wound-healing analysis (Fig. 4C). This is consistent with the fewer and defective lamellipodia seen in Pacsin 2 knockdown cells. Collectively, our data suggest that PC1 is an upstream component in the PC1-Pacsin 2-N-Wasp-Arp2/3-mediated actin assembly pathway.

PC1 and Pacsin 2 are required for the directional persistency during cell migration

To investigate the intrinsic migratory behavior of kidney epithelial cells, MEK DBA^{+} cells were seeded sparsely and monitored by time-lapse phase-contrast microscopy. Wild-type cells display a polarized phenotype with a dominant lamellipodium

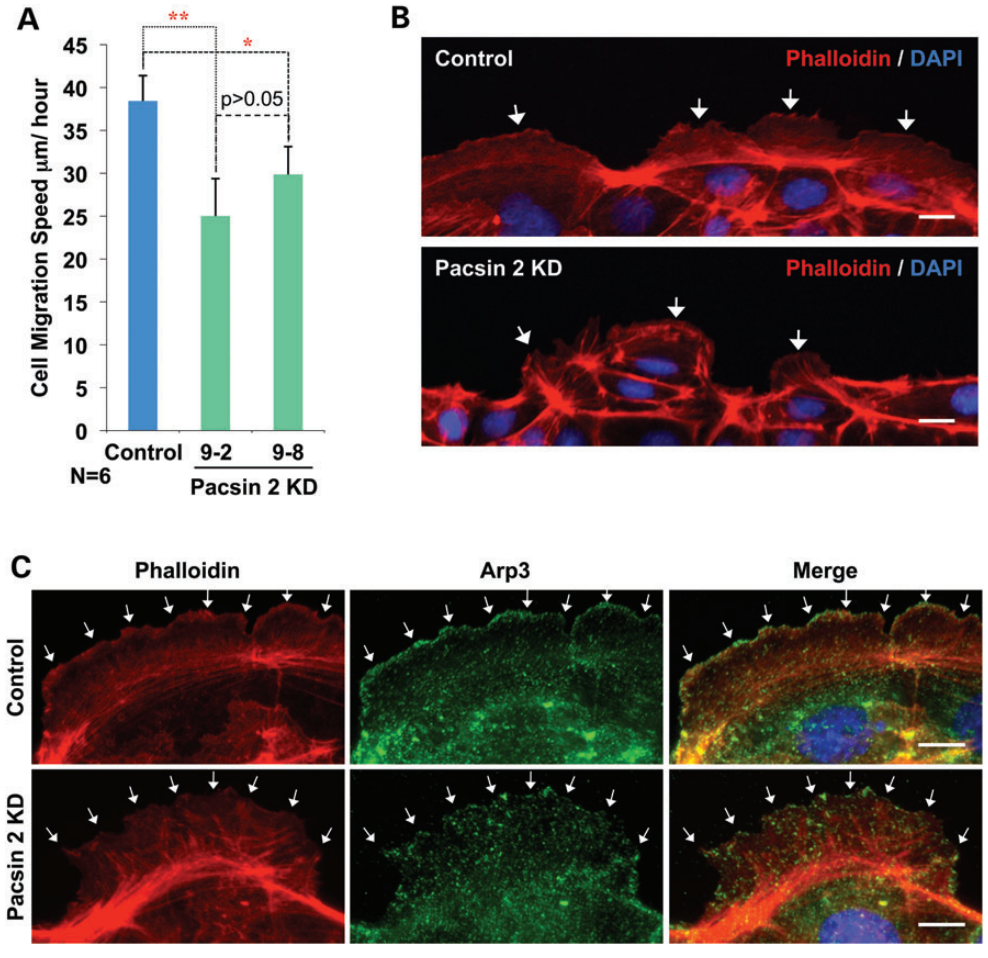

Figure 4 Pacsin 2 is required for kidney epithelial cell migration. (**A**) Comparison of cell migration speed between control and Pacsin 2 knockdown cells in the initial 6 h after scratching in six individual wound-healing experiments. (**B**) Five hours after scratching, Pacsin 2 knockdown mIMCD3 cells formed fewer, smaller lamellipodia when compared with control cells, as revealed by rhodamine-phalloidin staining of the actin cytoskeleton. Arrows point to the lamellipodia. (**C**) Five hours after scratching, fewer stress fibers and reduced Arp3 levels were found on the leading edge of the lamellipodia of Pacsin 2 knockdown mIMCD3 cells, as compared with control cells. The actin cytoskeleton was stained by rhodamine-phalloidin. Arrows point to the lamellipodia. Scale bar stands for 10 μm.

at the cell front and migrate to various directions. In agreement with the wound-healing experiment, *Pkd1*$^{null/null}$ cells migrate slower at 32.3 μm/h in contrast to wild-type cell, which migrate at 38.0 μm/h. *Pkd1*$^{null/null}$ cells frequently make turns, which results in a reduced directional persistency (0.51 for wild type, while 0.37 for *Pkd1*$^{null/null}$ cells) (as calculated by the ratio of the shortest linear direct distance from the start to the endpoint divided by the total track distance migrated by an individual cell). These PC1-deficient cells possess membrane protrusions that were retracted frequently during migration (Fig. 5A–C; Supplementary Material, Movies S1 and S2). Consistently, in the sparse cultures, Pacsin 2 knockdown cells also migrated with a reduced speed and directional persistency, compared with its control mIMCD3 cells (Fig. 5D and E; Supplementary Material, Movies S3 and S4).

DISCUSSION

Formation of a tubule with defined length and lumen diameter is a fundamental step for epithelial and endothelial cells to make many vital organs. ADPKD, the most common life-threatening monogenic disease that manifests itself in cyst formation in multiple epithelial organs, is the result of the loss of control of tubule lumen size. One of the prerequisites for proper tubulogenesis *in vitro* and *in vivo* is directional cell migration. Here, we have identified Pacsin 2 as a novel PC1-interacting protein and discovered a novel protein complex composed of PC1-Pacsin 2-N-Wasp. We show here that the PC1-Pacsin 2-N-Wasp protein complex modulates Arp2/3 complex function and controls the rate and direction of cell migration through modulating actin cytoskeleton. We further show for the first time that disorganization of actin cytoskeleton is a feature of ADPKD *in vivo*.

Lamellipodia formation through actin filament polymerization at the leading edge of a migrating cell provides the main motile force for the advancement of the cell's front and is the underlying process of the locomotion of mammalian cells (42,43). Both PC1 and Pacsin 2-deficient kidney epithelial cells migrate at a remarkably reduced speed during wound healing, with disrupted lamellipodia. Pacsin 2, via its SH3 domain, interacts with and activates N-Wasp (18), which in turn regulates the actin nucleation activity of the Arp2/3 complex (44). In this study, we show that Pacsin 2

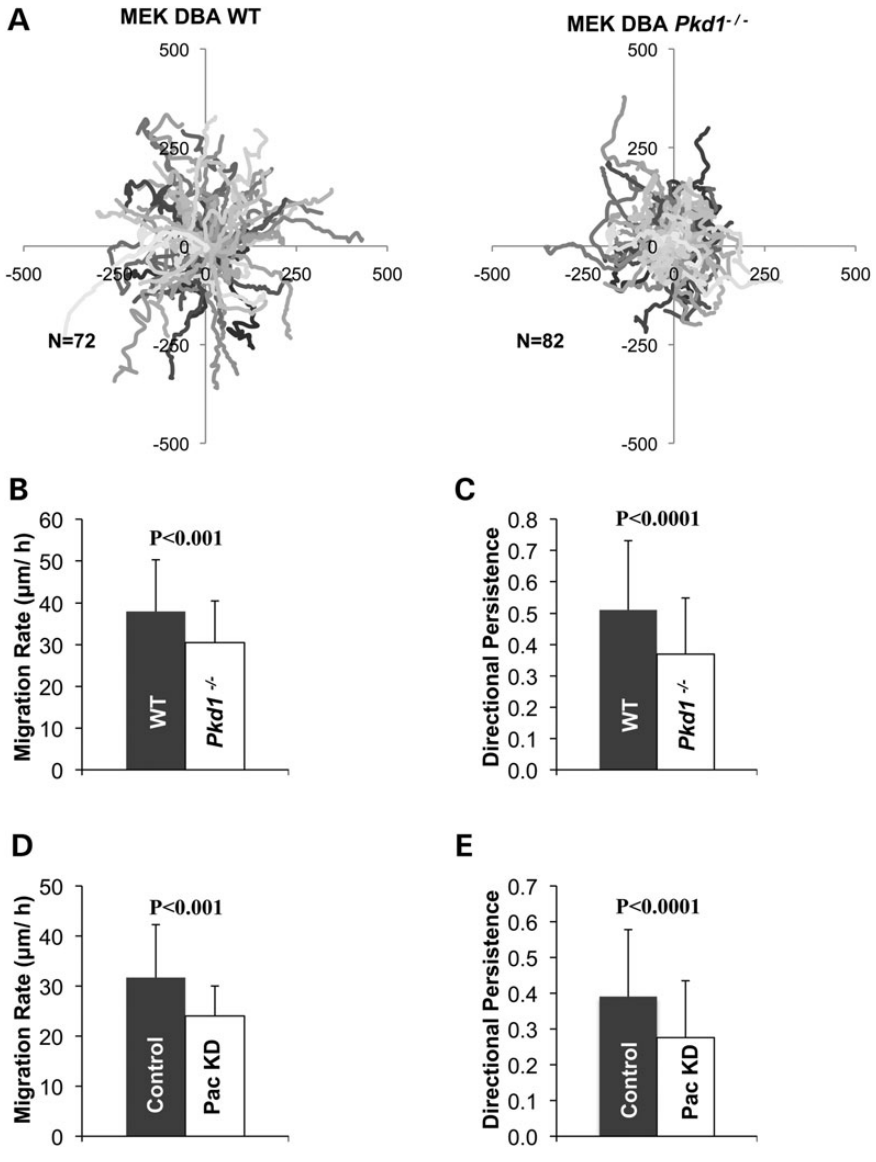

Figure 5 PC1 and Pacsin 2 are required for directional cell migration in kidney epithelial cells. All measurements are made for a 12-h period. (**A**) Migration track of wild-type (WT) and *Pkd1*$^{Null/Null}$ MEK DBA^{+} cells. Each line represents the migration path of one cell. The starting point of each cell migration was superimposed at the intersection of the *X* and *Y* axes. Cells that migrated <50 μm are excluded from this analysis as described for endothelial cells (41). (**B** and **C**) Quantitative analyses of data from (A). The *Pkd1*$^{Null/Null}$ cells migrated at a slower speed (B) with reduced directional persistency (C) compared with MEK DBA^{+} wild-type cells. Consistently, Pacsin 2-depleted mIMCD3 cells also migrated at a reduced speed (**D**) and directional persistency (**E**).

binds to the coiled-coil domain of PC1 through a 107-residue fragment containing the α3 helix of the F-BAR domain, Thus, we propose that Pacsin 2 acts as a scaffold protein holding both PC1 and N-Wasp in the same complex, and transduces the extracellular signals received by PC1 to active actin remodeling and subsequently controls cell migration and kidney tubule structure. This hypothesis is supported by the fact that all three proteins can be co-immunoprecipitated from different kidney epithelial cell lysates. The reduction of Arp3 in this protein complex following either PC1 or Pacsin 2 depletion suggests the requirement of both PC1 and Pacsin 2 for N-Wasp to regulate Arp2/3 complex actin nucleation activity. Consistently with this hypothesis, the levels of Arp3 and actin filaments are reduced in the lamellipodia of Pacsin 2-deficient cells during wound healing.

In the normal kidney, F-actin typically localizes to the apical and basal membranes of tubular epithelial cells. However, this apical–basal localization of F-actin is replaced by disorganized actin filaments in most cystic areas in *Pkd1*-deficient kidneys, indicating defective actin cytoskeleton organization, which may contribute to cyst formation and enlargement. In culture, PC1 mutant kidney epithelial cells display disorganized actin filaments, disrupted lamellipodia and reduced Pacsin 2 and Arp3 levels in the lamellipodia, especially in the active migrating cells. Taken together, we propose a model in which PC1 controls Arp3 activity through the PC1-Pacsin 2-N-Wasp interaction and subsequently modulates actin assembly and cell migration (Fig. 6). This model is further supported by our biochemical evidence, which demonstrates that pathogenic PC1 mutations in the

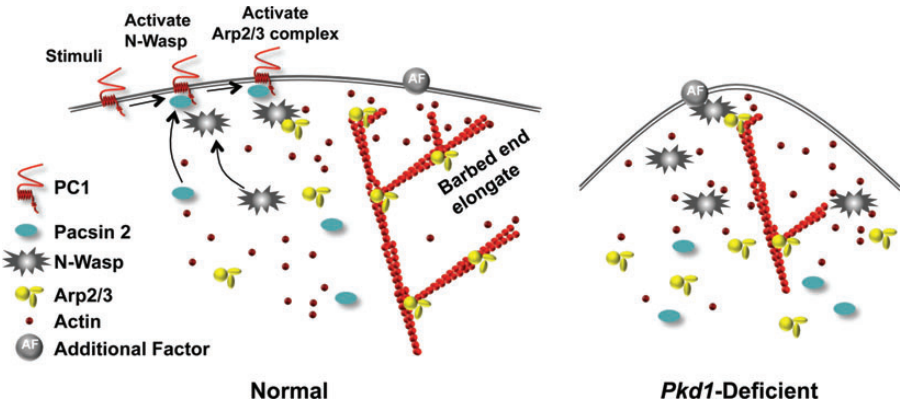

Figure 6 Schematic models of the PC1-Pacsin 2 protein complex regulating the actin cytoskeleton in a migrating cell. When cell migration is required, PC1 signals Pacsin 2 to the leading edge via an interaction of its cytoplasmic tail with the F-BAR domain of Pacsin 2. Pacsin 2 acts as a scaffold protein and further recruits N-Wasp via its SH3 domain. The PC1-Pacsin 2 complex activates N-Wasp and the latter promotes actin nucleation through the Arp2/3 complex. PC1 deficiency leads to a defect in the stabilization of the Arp2/3 complex at the leading edge of lamellipodia and a reduction in the rate of actin nucleation and cell migration speed. Additional factor(s) (AF) may also modulate this process.

coiled-coil domain or elsewhere severely impair the binding of PC1 to Pacsin 2.

Lamellipodia and filopodia at the protruding front of a migrating cell provide not only the main locomotion force but also directional persistency. Consistent with the slower migration and defective actin polymerization at the protruding front of kidney epithelial cells lacking either PC1 or Pacsin 2, live cell imaging showed that both cell types possess short-lived membrane protrusions that were retracted frequently during migration, which attribute to remarkably reduced directional persistency compared with their control cells and hence affecting intrinsic directionality.

Overexpressing PC1 proteins triggers cell migration and branching morphogenesis in MDCK and mIMCD3 cells (37,38), while silencing PC1 expression promotes cyst formation in mIMCD3 cells. N-Wasp deficiency also causes slower cell migration and reduced branching and tubule extension in tubulogenesis in 3D culture (36). In support with our proposed model here that Pacsin 2 is required for directional cell migration and consequently affects the renal tubulogenesis, we recently reported that Pacsin 2 has a distinct apical expression in the ureteric bud and its derived nephron segments in embryonic and postnatal mouse kidneys, where and when dynamic cell migration is needed for the formation and elongation of renal tubules (26). Moreover, silencing Pacsin 2 expression in mIMCD3 cells remarkably blocked tubule formation in an *in vitro* 3D culture system, and resulted in the formation of multiple lumen structures suggesting defective cell migration preventing proper tubule formation. Given the striking actin cytoskeleton defects seen in *Pkd1*-deficient cystic kidneys, these *in vitro* tubulogenesis migratory defects (26) further support a role for the PC1-Pacsin 2-N-Wasp complex in control of the actin cytoskeleton organization and tubular structure in the kidney.

Boca *et al.* showed that, by a scratch assay in PC1 overexpressing MDCK cells, there is an increase in Akt phosphorylation in scratched cells when compared with control cells. The authors proposed that PC1 modulates actin cytoskeleton rearrangement through PI3 kinase-dependent pathway (16). In this study, we found that consistent with the hyperactivation of AKT in ADPKD kidneys, basal levels of both total and phosphorylated AKT are elevated in *Pkd1*$^{null/null}$ cells compared with wild-type cells. However, unlike in PC1 overexpressing cells, scratch did not cause further Akt activation in PC1-deficient epithelial cells, compared with control cells. This may reflect a difference between PC1 deficiency and overexpression systems. We did not observe obvious difference in Akt activation between Pacsin 2 knockdown and control mIMCD3 cells after scratch either (Supplementary Material, Fig. S5).

Recently, Pacsin 2 has been shown to bind to Rac 1 (40), a small GTPase and cyclin D1 (39) in order to modulate cell migration. CDC42, another small GTPase which is upregulated in precystic in *Pkd1* knockout mice (45), also interacts and activates N-Wasp at the cell membrane and subsequently induces actin filament assembly in lamellipodia by the Arp2/3 complex. Therefore, the PC1-Pacsin 2-N-Wasp complex likely works together with additional factors to coordinate directional cell migration, and subsequently controls tubule geometry.

In summary, here we have identified Pacsin 2 as a novel PC1-interacting protein *in vitro* and *in vivo*. We demonstrate for the first time that disorganization of actin cytoskeleton is a feature of PKD *in vivo* and that a novel PC1-Pacsin 2-N-Wasp complex is required for the actin remodeling and directional cell migration. We propose that this protein complex contributes to the formation and maintenance of sophisticated normal kidney tubular structures and that mutations in PC1 impair the function of this protein complex, the organization of actin cytoskeleton, and directional cell migration, hence attributing to ADPKD pathobiology.

MATERIALS AND METHODS

Cell culture

mIMCD3 were purchased from ATCC (CRL-2123) and cultured in DMEM/F12 50/50 supplemented with 10% fetal bovine serum. MEK cells, developed in our laboratory, were derived from embryonic Day 15.5 kidneys from wild-type and *Pkd1*$^{null/null}$ mice bearing temperature-sensitive simian virus 40 large T antigen.

MEK cells were usually cultured at 33°C in simian virus 40 epithelium media and were transferred to 37°C and withdrawal of interferon for 3–4 days for differentiation (46).

The stable Pacsin 2 knockdown and its scrambled control mIMCD3 cell lines were established in our laboratory (26). Briefly, the pSilencer 2.1-U6-Neo-Pacsin 2 shRNA plasmid was transfected into mIMCD3 cells with lipofectamine 2000 (Invitrogen). The mouse Pacsin 2 shRNA target sequence is 5′-ATGTCTGTCACCT ACGATG-3′. As a control, the pSilencer 2.1-U6-Neo plasmid (Ambion) encoding a small hairpin shRNA which shows no homology to any known gene was also transfected into cells. Cells were selected using 1 mg/ml G418 in growth media for 20 days. Surviving clones were picked individually. The knockdown efficiency was confirmed by western blotting and semi-quantitative-PCR analyses.

Western analysis

Briefly, the protein samples were electrophoresed on SDS-acrylamide resolving gels and transferred to Hybond ECL nitrocellulose membranes. After being blocked with 5% non-fat dry milk in PBS, the filters were incubated with the primary antibody either 1 h at room temperature or overnight in a cold room and washed three times with PBS-0.1% Tween 20. The filters were finally incubated with a horseradish peroxidase-linked secondary antibody. After being washed thoroughly, the bound antibodies were detected with the ECL western-blot analysis system. If needed, the same filter was stripped with restore western-blot stripping buffer and re-blotted according to the protocol provided by Pierce.

Primary antibodies for western blotting are the following: anti-Pacsin 2 (18) 1:15 000 dilution, anti-PC1 (Santa Cruz Biotechnology, Inc. 7E12 sc-130557 1:1000 dilution, anti-N-Wasp (Santa Cruz Biotechnology, Inc. H-100 sc-20770 and 93-W sc-100964) 1:500 dilution, anti-Arp3 (Abcam Inc. ab49671) 1:5000 dilution, anti-GST (Santa Cruz Biotechnology, Inc. Z5 sc-459) 1:2000 dilution and anti-GAPDH (Santa Cruz Biotechnology, Inc. FL-335 sc-25778) 1:1000 dilution. Secondary antibodies (Amersham Pharmacia Biotech) were used at 1:5000 dilution.

GST pull-down assay

GST and the GST fusion proteins were generated as previously described (28). In brief, proteins were expressed in the *Escherichia coli* BL21 cells. The bacteria were grown in selective medium containing 2% glucose to an A600 of 0.8 at 37°C, followed by induction with either 0.1 or 1 mM isopropyl β-D-1-thiogalactopyranoside at 30°C for another 2 h. Cells were harvested by centrifugation and re-suspended in a PBS solution containing 5 mM DTT, 1 mg/ml lysozyme and protease inhibitors, followed by sonication on ice. The GST fusion proteins were purified from these cell lysates by binding the fusion proteins to Glutathione Sepharose 4B beads in accordance with the manufacturer's instructions (Amersham Pharmacia Biotech). Cell lysates were incubated with GST fusion proteins immobilized on Glutathione–Sepharose beads (Amersham Pharmacia Biotech) at 4°C overnight.

The beads were centrifuged and were washed five times with ice-cold PBS washing buffer with 0.05% Triton X-100. The washed beads were solubilized in an equal volume of 2× SDS sample buffer and proteins eluted by boiling for 5 min and analyzed by western blotting.

Co-immunoprecipitation

MEK and/or mIMCD3 cells were homogenized with M-PER (Pierce) containing protease inhibitors (Roche) and 1 mM DTT. For co-immunoprecipitation, 2–4 mg of the cell lysates (protein concentrations were >5 mg/ml) were incubated with either 2–4 μg antibodies or an equal amount of normal rabbit IgG with gentle rocking overnight at 4°C. Protein A Sepharose beads (Invitrogen) were added and incubated for another 2 h at 4°C. The washed beads were solubilized in an equal volume of 2× SDS sample buffer and proteins were eluted by boiling for 5 min and analyzed by western blotting.

Immunostaining and immunofluorescence microscopy

Cultured cells were fixed with 4% paraformaldehyde −3% sucrose and permeabilized with 0.3% Triton X-100. Permeabilized cells were blocked with either 5% BSA or 10% goat serum for 1 h at room temperature and then incubated with the primary antibodies for 1 h at room temperature or overnight at 4°C. After completely washing with ice-cold PBS, they were incubated with a labeled secondary antibody for 1 h at room temperature. Slides were mounted with ProLong® Gold anti-fade reagent with DAPI (Invitrogen, Catalog # P36935). A Nikon fluorescence microscope and the SPOT camera system were used for image analysis (Nikon, Tokyo, Japan).

Paraffin-embedded sections (4 μm), derived from perfused kidneys, were dewaxed, rehydrated through graded alcohols and boiled in 10 mM citrate (pH 6.0) (Vector laboratories, CA, USA) for 30 min. The sections were then placed in the staining dish at room temperature, allowed to cool for 1–2 h, and blocked with 5% BSA or 10% goat serum for 1 h at room temperature. The sections were then processed as cultured cells as mentioned above.

For phalloidin staining of actin cytoskeleton in the kidney, OCT-embedded cryosections (10 μm) of PBS perfused kidneys, were blocked with 5% BSA for 1 h at room temperature, and then incubated with rhodamine-labeled phalloidin (Invitrogen, Catalog # R415) 1:500 dilution for 1 h at room temperature. Slides were mounted with ProLong® Gold anti-fade reagent with DAPI (Invitrogen, Catalog # P36935). A confocal Nikon microscope was used for image analysis (Nikon, Tokyo, Japan).

Primary antibodies for immunostaining are the following: Pacsin 2 (18) 1:4000 dilution; GFP (COVANCE MMS-118P) 1:5000 dilution, Arp3 (Abcam Inc. ab49671) 1:1000 dilution, Rhodamine Phalloidin (Invitrogen R415) 1:500 dilution, anti-acetylated-α-tubulin (Sigma-Aldrich, MO, USA, Catalog # T6793) 1:40 000 dilution, fluorescent-labeled second antibodies were all from Invitrogen and used at 1:500 dilution.

Wound-healing assay

Cells were seeded at confluence and cultured for an additional 24 h on collagen type I-coated 6-well culture dishes. Wounds were induced by scratching the cell monolayer with a sterile 200-μl pipette tip. Images were captured by phase-contrast microscopy immediately following wound induction (0 h), and at

3, 6 and 9 h post-scratching. A single wound was induced per experiment. To quantify cellular migration across the width of the wound, the distance (in μm) throughout the wound was measured at each time point (in six individual wells per experiment). Data are presented as the cell migration speed from 0 h (time of wound induction) to 6 h post-wounding.

Live cell imaging analysis

To analyze the intrinsic migratory behavior of kidney epithelial cells, ∼500 cells were seeded sparsely on type I collagen coated 6-well dishes. Phase-contrast images were collected using 10× objective lenses at every 15 min for a period of 24 h with a CCD video camera (Nikon). Cells were tracked with NIS Element software to quantify migratory parameters including the migration distance, rate, path and directional persistence. For tracing random cell migration, cells were manually tracked for each frame based on the central position of the nuclei. All cells analyzed have to migrate a distance of 50 μm or more from the starting point during 12 h in each experiment as described previously (41). To exclude the effect of cell division and cell contact, we only analyzed non-dividing cells without cell–cell contact during the 12 h of experiments. Directional persistence was represented by the ratio of the shortest linear direct distance from the start to the endpoint divided by the total track distance migrated by an individual cell. Migration rate was defined by the total distance traveled divided by time and expressed in units of μm/h. Based on the coordinates obtained from the translocation of the nuclei of the cells, graphical representations of the migratory paths were generated using Excel for visualization.

SUPPLEMENTARY MATERIAL

Supplementary Material is available at *HMG* online.

ACKNOWLEDGEMENTS

We thank the members of the Zhou Lab and the Harvard Center for Polycystic Kidney Disease Research (P50DK074030) for scientific discussions and support. We also thank Drs C. Ward and P. Harris for providing us 7e12 antibody.

Conflict of Interest statement. None declared.

FUNDING

This work was supported by grants from the National Institutes of Health (DK51050, DK40703 and P50DK074030) to J.Z. G.Y. is a recipient of a postdoctoral fellowship from the American Heart Association.

REFERENCES

1. Gabow, P.A. (1993) Autosomal dominant polycystic kidney disease. *N. Engl. J. Med.*, **329**, 332–342.
2. Zhou, J. and Pei, Y. (2007) *Autosomal Dominant Polycystic Kidney Disease*. Elsevier, 85–171.
3. Zhou, J. (2009) Polycystins and primary cilia: primers for cell cycle progression. *Annu. Rev. Physiol.*, **71**, 83–113.
4. Reeders, S.T., Breuning, M.H., Davies, K.E., Nicholls, R.D., Jarman, A.P., Higgs, D.R., Pearson, P.L. and Weatherall, D.J. (1985) A highly polymorphic DNA marker linked to adult polycystic kidney disease on chromosome 16. *Nature*, **317**, 542–544.
5. Consortium, T.I.P.K.D. (1995) Polycystic kidney disease: the complete structure of the PKD1 gene and its protein. The International Polycystic Kidney Disease Consortium. *Cell*, **81**, 289–298.
6. Hughes, J., Ward, C.J., Peral, B., Aspinwall, R., Clark, K., San Millan, J.L., Gamble, V. and Harris, P.C. (1995) The polycystic kidney disease 1 (PKD1) gene encodes a novel protein with multiple cell recognition domains. *Nat. Genet.*, **10**, 151–160.
7. Weston, B.S., Bagneris, C., Price, R.G. and Stirling, J.L. (2001) The polycystin-1 C-type lectin domain binds carbohydrate in a calcium-dependent manner, and interacts with extracellular matrix proteins *in vitro*. *Biochim. Biophys. Acta*, **1536**, 161–176.
8. Malhas, A.N., Abuknesha, R.A. and Price, R.G. (2002) Interaction of the leucine-rich repeats of polycystin-1 with extracellular matrix proteins: possible role in cell proliferation. *J. Am. Soc. Nephrol.*, **13**, 19–26.
9. Parnell, S.C., Magenheimer, B.S., Maser, R.L. and Calvet, J.P. (1999) Identification of the major site of *in vitro* PKA phosphorylation in the polycystin-1 C-terminal cytosolic domain. *Biochem. Biophys. Res. Commun.*, **259**, 539–543.
10. Parnell, S.C., Magenheimer, B.S., Maser, R.L., Rankin, C.A., Smine, A., Okamoto, T. and Calvet, J.P. (1998) The polycystic kidney disease-1 protein, polycystin-1, binds and activates heterotrimeric G-proteins *in vitro*. *Biochem. Biophys. Res. Commun.*, **251**, 625–631.
11. Li, H.P., Geng, L., Burrow, C.R. and Wilson, P.D. (1999) Identification of phosphorylation sites in the PKD1-encoded protein C-terminal domain. *Biochem. Biophys. Res. Commun.*, **259**, 356–363.
12. Hanaoka, K., Qian, F., Boletta, A., Bhunia, A.K., Piontek, K., Tsiokas, L., Sukhatme, V.P., Guggino, W.B. and Germino, G.G. (2000) Co-assembly of polycystin-1 and -2 produces unique cation-permeable currents. *Nature*, **408**, 990–994.
13. Delmas, P., Nomura, H., Li, X., Lakkis, M., Luo, Y., Segal, Y., Fernandez-Fernandez, J.M., Harris, P., Frischauf, A.M., Brown, D.A. *et al.* (2002) Constitutive activation of G-proteins by polycystin-1 is antagonized by polycystin-2. *J. Biol. Chem.*, **277**, 11276–11283.
14. Geng, L., Segal, Y., Peissel, B., Deng, N., Pei, Y., Carone, F., Rennke, H.G., Glucksmann-Kuis, A.M., Schneider, M.C., Ericsson, M. *et al.* (1996) Identification and localization of polycystin, the PKD1 gene product. *J. Clin. Invest.*, **98**, 2674–2682.
15. Geng, L., Segal, Y., Pavlova, A., Barros, E.J., Lohning, C., Lu, W., Nigam, S.K., Frischauf, A.M., Reeders, S.T. and Zhou, J. (1997) Distribution and developmentally regulated expression of murine polycystin. *Am. J. Physiol.*, **272**, F451–F459.
16. Boca, M., D'Amato, L., Distefano, G., Polishchuk, R.S., Germino, G.G. and Boletta, A. (2007) Polycystin-1 induces cell migration by regulating phosphatidylinositol 3-kinase-dependent cytoskeletal rearrangements and GSK3beta-dependent cell cell mechanical adhesion. *Mol. Biol. Cell*, **18**, 4050–4061.
17. Ritter, B., Modregger, J., Paulsson, M. and Plomann, M. (1999) PACSIN 2, a novel member of the PACSIN family of cytoplasmic adapter proteins. *FEBS Lett.*, **454**, 356–362.
18. Modregger, J., Ritter, B., Witter, B., Paulsson, M. and Plomann, M. (2000) All three PACSIN isoforms bind to endocytic proteins and inhibit endocytosis. *J. Cell Sci.*, **113**, 4511–4521.
19. Kessels, M.M. and Qualmann, B. (2004) The syndapin protein family: linking membrane trafficking with the cytoskeleton. *J. Cell Sci.*, **117**, 3077–3086.
20. Qualmann, B. and Kelly, R.B. (2000) Syndapin isoforms participate in receptor-mediated endocytosis and actin organization. *J. Cell Biol.*, **148**, 1047–1062.
21. Merrifield, C.J., Feldman, M.E., Wan, L. and Almers, W. (2002) Imaging actin and dynamin recruitment during invagination of single clathrin-coated pits. *Nat. Cell Biol.*, **4**, 691–698.
22. Kessels, M.M. and Qualmann, B. (2002) Syndapins integrate N-WASP in receptor-mediated endocytosis. *EMBO J.*, **21**, 6083–6094.
23. Baum, B. and Kunda, P. (2005) Actin nucleation: spire – actin nucleator in a class of its own. *Curr. Biol.*, **15**, R305–R308.
24. Cousin, H., Desimone, D.W. and Alfandari, D. (2008) PACSIN2 regulates cell adhesion during gastrulation in Xenopus laevis. *Dev. Biol.*, **319**, 86–99.
25. Edeling, M.A., Sanker, S., Shima, T., Umasankar, P.K., Honing, S., Kim, H.Y., Davidson, L.A., Watkins, S.C., Tsang, M., Owen, D.J. *et al.* (2009)

Structural requirements for PACSIN/Syndapin operation during zebrafish embryonic notochord development. *PLoS ONE*, **4**, e8150.
26. Yao, G., Luyten, A., Takakura, A., Plomann, M. and Zhou, J. (2012) The cytoplasmic protein Pacsin 2 in kidney development and injury repair. *Kidney Int.*, **83**, 426–437.
27. Plomann, M., Wittmann, J.G. and Rudolph, M.G. (2010) A hinge in the distal end of the PACSIN 2 F-BAR domain may contribute to membrane-curvature sensing. *J. Mol. Biol.*, **400**, 129–136.
28. Yuasa, T., Takakura, A., Denker, B.M., Venugopal, B. and Zhou, J. (2004) Polycystin-1L2 is a novel G-protein-binding protein. *Genomics*, **84**, 126–138.
29. Li, X., Luo, Y., Starremans, P.G., McNamara, C.A., Pei, Y. and Zhou, J. (2005) Polycystin-1 and polycystin-2 regulate the cell cycle through the helix-loop-helix inhibitor Id2. [erratum appears in Nat Cell Biol. 2006 Jan;8(1):100]. *Nat. Cell Biol.*, **7**, 1202–1212.
30. Luo, Y., Vassilev, P.M., Li, X., Kawanabe, Y. and Zhou, J. (2003) Native polycystin 2 functions as a plasma membrane Ca2+-permeable cation channel in renal epithelia. *Mol. Cell. Biol.*, **23**, 2600–2607.
31. Hopp, K., Ward, C.J., Hommerding, C.J., Nasr, S.H., Tuan, H.F., Gainullin, V.G., Rossetti, S., Torres, V.E. and Harris, P.C. (2012) Functional polycystin-1 dosage governs autosomal dominant polycystic kidney disease severity. *J. Clin. Invest.*, **122**, 4257–4273.
32. Badenas, C., Torra, R., San Millan, J.L., Lucero, L., Mila, M., Estivill, X. and Darnell, A. (1999) Mutational analysis within the 3' region of the PKD1 gene. *Kidney Int.*, **55**, 1225–1233.
33. Rossetti, S., Kubly, V.J., Consugar, M.B., Hopp, K., Roy, S., Horsley, S.W., Chauveau, D., Rees, L., Barratt, T.M., van't Hoff, W.G. *et al.* (2009) Incompletely penetrant PKD1 alleles suggest a role for gene dosage in cyst initiation in polycystic kidney disease. *Kidney Int.*, **75**, 848–855.
34. Chapin, H.C., Rajendran, V. and Caplan, M.J. (2010) Polycystin-1 surface localization is stimulated by polycystin-2 and cleavage at the G protein-coupled receptor proteolytic site. *Mol. Biol. Cell*, **21**, 4338–4348.
35. Subramanian, B., Rudym, D., Cannizzaro, C., Perrone, R., Zhou, J. and Kaplan, D.L. (2010) Tissue-engineered three-dimensional *in vitro* models for normal and diseased kidney. *Tissue Eng. A*, **16**, 2821–2831.
36. Yamaguchi, H., Miki, H. and Takenawa, T. (2002) Neural Wiskott-Aldrich syndrome protein is involved in hepatocyte growth factor-induced migration, invasion, and tubulogenesis of epithelial cells. *Cancer Res.*, **62**, 2503–2509.
37. Boletta, A., Qian, F., Onuchic, L.F., Bhunia, A.K., Phakdeekitcharoen, B., Hanaoka, K., Guggino, W., Monaco, L. and Germino, G.G. (2000) Polycystin-1, the gene product of PKD1, induces resistance to apoptosis and spontaneous tubulogenesis in MDCK cells. *Mol. Cell*, **6**, 1267–1273.
38. Nickel, C., Benzing, T., Sellin, L., Gerke, P., Karihaloo, A., Liu, Z.X., Cantley, L.G. and Walz, G. (2002) The polycystin-1 C-terminal fragment triggers branching morphogenesis and migration of tubular kidney epithelial cells. *J. Clin. Invest.*, **109**, 481–489.
39. Meng, H., Tian, L., Zhou, J., Li, Z., Jiao, X., Li, W.W., Plomann, M., Xu, Z., Lisanti, M.P., Wang, C. *et al.* (2011) PACSIN 2 represses cellular migration through direct association with cyclin D1 but not its alternate splice form cyclin D1b. *Cell Cycle*, **10**, 73–81.
40. de Kreuk, B.J., Nethe, M., Fernandez-Borja, M., Anthony, E.C., Hensbergen, P.J., Deelder, A.M., Plomann, M. and Hordijk, P.L. (2011) The F-BAR domain protein PACSIN2 associates with Rac1 and regulates cell spreading and migration. *J. Cell Sci.*, **124**, 2375–2388.
41. Wojciak-Stothard, B. and Ridley, A.J. (2003) Shear stress-induced endothelial cell polarization is mediated by Rho and Rac but not Cdc42 or PI 3-kinases. *J. Cell Biol.*, **161**, 429–439.
42. Mitchison, T.J. and Cramer, L.P. (1996) Actin-based cell motility and cell locomotion. *Cell*, **84**, 371–379.
43. Pollard, T.D. and Borisy, G.G. (2003) Cellular motility driven by assembly and disassembly of actin filaments. *Cell*, **112**, 453–465.
44. Rohatgi, R., Ma, L., Miki, H., Lopez, M., Kirchhausen, T., Takenawa, T. and Kirschner, M.W. (1999) The interaction between N-WASP and the Arp2/3 complex links Cdc42-dependent signals to actin assembly. *Cell*, **97**, 221–231.
45. Luyten, A., Su, X., Gondela, S., Chen, Y., Rompani, S., Takakura, A. and Zhou, A.J. (2010) Aberrant regulation of planar cell polarity in polycystic kidney disease. *J. Am. Soc. Nephrol.*, **21**, 1521–1532.
46. Nauli, S.M., Alenghat, F.J., Luo, Y., Williams, E., Vassilev, P., Li, X., Elia, A.E., Lu, W., Brown, E.M., Quinn, S.J. *et al.* (2003) Polycystins 1 and 2 mediate mechanosensation in the primary cilium of kidney cells.[see comment]. *Nat. Genet.*, **33**, 129–137.